Progress In Electromagnetics Research B, Vol. 32, 75–90, 2011

WAVEGUIDES FILLED WITH BILAYERS OF DOUBLE-NEGATIVE (DNG) AND DOUBLE-POSITIVE (DPS) METAMATERIALS

E. Cojocaru*

Department of Theoretical Physics, Horia Hulubei National Institute of Physics and Nuclear Engineering, P. O. Box MG-6, Magurele, Bucharest 077125, Romania

Abstract—Simple normalized dispersion relations for transverse magnetic (TM) and transverse electric (TE) propagating modes in parallel-plate waveguides filled with DPS/DPS or DNG/DNG, and DNG/DPS bilayers are presented. The evanescent TE_0 mode of the waveguide filled with a DNG/DPS bilayer is characterized also by a simple normalized dispersion relation. Since an important behavior of the modes in the waveguide filled with a DNG/DPS bilayer is the existence of a turning point (TP) at which the power carried by the respective mode on the propagation direction equals zero and changes the sign, we present also implicit relations for determining the normalized parameters of the TM and TE modes at that TP. We show that the TP begins to exist at certain values of the normalized parameter v_2 characterizing the DPS layer. For both the TM and TE modes, the higher is the mode order, the greater is the v_2 parameter at which the TP begins to exist, but the behavior of the TP is different for the TM and TE modes.

1. INTRODUCTION

The double-negative (DNG) materials having both negative permittivity and negative permeability, enjoy an increased interest, especially because of their physical properties which are different from those of the conventional double-positive (DPS) materials. Veselago [1] was the first to study theoretically the DNG materials. Various aspects of this class of metamaterials have been studied for example in [2–22].

Interesting characteristics of the guided modes in the parallel-plate waveguides filled with bilayers of DPS and DNG materials have

Received 6 May 2011, Accepted 30 June 2011, Scheduled 6 July 2011

* Corresponding author: E. Cojocaru (ecojocaru@theory.nipne.ro).

been revealed previously in [9, 13] but in terms of different physical parameters. In this paper we present simple normalized dispersion relations for the guided or evanescent modes in the parallel-plate waveguides filled with DPS/DPS, or DNG/DNG, and DNG/DPS bilayers. Numerical examples are given showing dispersion curves of the lower order modes and the total normalized power carried on the propagation direction by the respective modes. Examples of electromagnetic fields inside the waveguide are also given.

It has been shown in [9, 15] that an important behavior of the modes in a grounded DNG slab and in the parallel-plate waveguide filled with a DNG/DPS bilayer is the existence of a turning point (TP) at which the power carried by each mode of order $m > 0$ equals zero and changes the sign. In this paper we present implicit relations for determining the normalized parameters at that TP for the guided modes in the parallel-plate waveguide filled with a DNG/DPS bilayer. Behaviors of the TPs are outlined by numerical examples.

2. GENERAL RELATIONS

We consider a parallel-plate waveguide, made of two infinitely extent perfectly electric conducting plates separated by the distance $d = d_1 + d_2$, as shown in Fig. 1. The waveguide is filled with a pair of parallel layers made of DNG and DPS materials. The two layers are characterized by their thicknesses d_1 and d_2, and the relative constitutive parameters (ϵ_1, μ_1) and (ϵ_2, μ_2), which are assumed real, nondispersive, and nondimensional, with $\epsilon_1\mu_1 > \epsilon_2\mu_2$. A monochromatic time-harmonic variation $\exp(i\omega t)$ is assumed. The z axis is chosen as direction of propagation of the guided modes whose electromagnetic field varies as $\exp[i(\omega t - \beta z)]$, where β is the modal phase constant. For transversal magnetic (TM) modes, the magnetic field is along the y direction, whereas it is the electric field along the

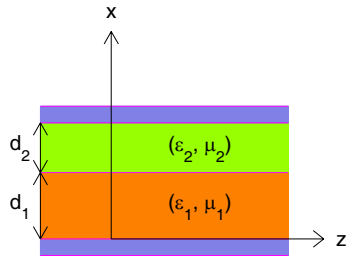

Figure 1. Geometry of the parallel-plate waveguide filled with a bilayer of relative material constants (ϵ_1, μ_1) and (ϵ_2, μ_2).

y direction in the case of transversal electric (TE) modes. Thus, the magnetic field H_y for the TM modes takes the form

$$H_y = \begin{cases} \cos(k_{t1}x) & \text{for } 0 < x < d_1 \\ A\cos[k_{t2}(x-d_1)] + B\sin[k_{t2}(x-d_1)] & \text{for } d_1 < x < d_1+d_2 \end{cases} \quad (1)$$

where the factor $\exp(-i\beta z)$ is skipped, and

$$A = \cos(k_{t1}d_1), \qquad B = -\frac{k_{t1}\epsilon_2}{k_{t2}\epsilon_1}\sin(k_{t1}d_1) \quad (2)$$

Similarly, the electric field E_y for the TE modes takes the form

$$E_y = \begin{cases} \sin(k_{t1}x) & \text{for } 0 < x < d_1 \\ A\sin[k_{t2}(x-d_1)] + B\cos[k_{t2}(x-d_1)] & \text{for } d_1 < x < d_1+d_2 \end{cases} \quad (3)$$

where the factor $\exp(-i\beta z)$ is skipped, and

$$A = \frac{k_{t1}\mu_2}{k_{t2}\mu_1}\cos(k_{t1}d_1), \qquad B = \sin(k_{t1}d_1) \quad (4)$$

where k_{tj}, with $j = 1, 2$, is defined by relation

$$k_{tj} = \begin{cases} \sqrt{k_0^2\epsilon_j\mu_j - \beta^2} & \text{when } \bar{\beta}^2 < \epsilon_j\mu_j \\ -i\sqrt{\beta^2 - k_0^2\epsilon_j\mu_j} & \text{when } \bar{\beta}^2 > \epsilon_j\mu_j \end{cases} \quad (5)$$

$\bar{\beta} = \beta/k_0$ is the relative phase constant, $k_0 = \omega\sqrt{\epsilon_0\mu_0}$ is the wavenumber in vacuum. The total normalized power carried by each mode on the z direction takes the form

$$\bar{P} = (P_1 + P_2)/(|P_1| + |P_2|) \quad (6)$$

where P_1 and P_2 are given up to a common factor by

$$P_1 \propto \frac{1}{\epsilon_1}\int_0^{d_1} |H_y|^2 \mathrm{d}x, \qquad P_2 \propto \frac{1}{\epsilon_2}\int_{d_1}^{d_1+d_2} |H_y|^2 \mathrm{d}x, \quad (7)$$

for the TM modes, and similarly

$$P_1 \propto \frac{1}{\mu_1}\int_0^{d_1} |E_y|^2 \mathrm{d}x, \qquad P_2 \propto \frac{1}{\mu_2}\int_{d_1}^{d_1+d_2} |E_y|^2 \mathrm{d}x \quad (8)$$

for the TE modes.

3. DISPERSION RELATIONS

Dispersion relations are determined either by applying the boundary conditions of the tangential electromagnetic fields at interfaces or from the poles of the complex amplitude reflection coefficients expressed in terms of the transfer matrix elements [23], taking into account that the perfectly electric conducting plates of the waveguide are characterized by an infinite permittivity and zero permeability [24].

3.1. The Case $\bar{\beta}^2 < \epsilon_2\mu_2 < \epsilon_1\mu_1$

The following dispersion relation results [9, 13]

$$\frac{k_{t1}}{\epsilon_1}\tan(k_{t1}d_1) + \frac{k_{t2}}{\epsilon_2}\tan(k_{t2}d_2) = 0 \tag{9}$$

for TM modes, and

$$\frac{\mu_1}{k_{t1}}\tan(k_{t1}d_1) + \frac{\mu_2}{k_{t2}}\tan(k_{t2}d_2) = 0 \tag{10}$$

for TE modes. Here we introduce the normalized parameters

$$v_j = k_0 d_j, \qquad u_j = \sqrt{\epsilon_j\mu_j - \bar{\beta}^2}, \qquad j = 1, 2 \tag{11}$$

Using relation (11) in (9) and (10) gives

$$\frac{\epsilon_1}{\epsilon_2}\tan(u_2v_2) + \frac{u_1}{u_2}\tan(u_1v_1) = 0 \tag{12}$$

for TM modes, and

$$\frac{\mu_1}{\mu_2}\tan(u_1v_1) + \frac{u_1}{u_2}\tan(u_2v_2) = 0 \tag{13}$$

for TE modes. The normalized dispersion relation of the guided modes is

$$v_1 = (1/u_1)\left\{\tan^{-1}\left[\gamma\tan(u_2v_2)\right] + m\pi\right\}, \qquad m = 0, 1, 2, \ldots \tag{14}$$

where

$$\gamma = \begin{cases} -\epsilon_1u_2/(\epsilon_2u_1) & \text{for } TM \text{ modes} \\ -\mu_2u_1/(\mu_1u_2) & \text{for } TE \text{ modes} \end{cases} \tag{15}$$

Note that, for simplicity, we label the modes by m without any reference to the standard mode labeling of DPS slabs. The cutoff $\bar{\beta} = 0$ is determined from (14),

$$v_1 = (1/\sqrt{\epsilon_1\mu_1})\left\{\tan^{-1}[\gamma_c\tan(v_2\sqrt{\epsilon_2\mu_2})] + m\pi\right\} \tag{16}$$

where

$$\gamma_c = \begin{cases} -\epsilon_1\sqrt{\epsilon_2\mu_2}/(\epsilon_2\sqrt{\epsilon_1\mu_1}) & \text{for } TM \text{ modes} \\ -\mu_2\sqrt{\epsilon_1\mu_1}/(\mu_1\sqrt{\epsilon_2\mu_2}) & \text{for } TE \text{ modes} \end{cases} \tag{17}$$

From relations (12) and (13) one can see that the cutoff $v_1 = 0$, when it exists, is determined by $u_2v_2 = l\pi$ for the TM and TE modes, where

l is an integer number. Thus, when the cutoff $v_1 = 0$ exists, it is determined by relation

$$\bar{\beta} = \sqrt{\epsilon_2\mu_2 - l^2\pi^2/v_2^2} \tag{18}$$

for the TM and TE modes. From relations (12) and (13) one can see also that when $u_1v_1 = u_2v_2$, a nondispersive mode [9, 13] exists in the waveguide filled with a DNG/DPS bilayer, which satisfies the relation

$$\epsilon_1/\epsilon_2 + u_1/u_2 = 0 \tag{19}$$

for the TM mode, and

$$\mu_1/\mu_2 + u_1/u_2 = 0 \tag{20}$$

for the TE mode.

3.2. The Case $\epsilon_2\mu_2 < \bar{\beta}^2 < \epsilon_1\mu_1$

In this case, k_{t2} in (5) is imaginary, and

$$k_{t2}d_2 = -ik_0d_2\sqrt{\bar{\beta}^2 - \epsilon_2\mu_2} = -iv_2\widetilde{u}_2 \tag{21}$$

where

$$\widetilde{u}_2 = \sqrt{\bar{\beta}^2 - \epsilon_2\mu_2} \tag{22}$$

The normalized dispersion relation of the guided modes is

$$v_1 = (1/u_1)\left\{\tan^{-1}[\widetilde{\gamma}\tanh(\widetilde{u}_2v_2)] + m\pi\right\} \tag{23}$$

where

$$\widetilde{\gamma} = \begin{cases} \epsilon_1\widetilde{u}_2/(\epsilon_2u_1) & \text{for } TM \text{ modes} \\ -\mu_2u_1/(\mu_1\widetilde{u}_2) & \text{for } TE \text{ modes} \end{cases} \tag{24}$$

3.3. The Case $\bar{\beta}^2 > \epsilon_1\mu_1 > \epsilon_2\mu_2$

In this case, k_{t1} and k_{t2} in (5) are imaginary, but in the parallel-plate waveguide filled with a DNG/DPS bilayer there is a TE_0 mode with real values of $\bar{\beta}$ [9, 13]. At $\bar{\beta}^2 = \epsilon_1\mu_1$, v_1 is determined by relation

$$v_1 = -(\mu_2/\mu_1)\tanh(v_2\sqrt{\epsilon_1\mu_1 - \epsilon_2\mu_2})/\sqrt{\epsilon_1\mu_1 - \epsilon_2\mu_2} \tag{25}$$

The mode TE_0 is evanescent and satisfies the normalized dispersion relation

$$v_1 = (1/\widetilde{u}_1)\tanh^{-1}\left[-\mu_2\widetilde{u}_1/(\mu_1\widetilde{u}_2)\tanh(\widetilde{u}_2v_2)\right] \tag{26}$$

where $\widetilde{u}_2$ is defined by (22) and $\widetilde{u}_1$ is defined similarly. Since μ_1 has negative values, v_1 in (26) has real values, with $v_1 \to 0$ when $\bar{\beta} \to \infty$.

4. NUMERICAL EXAMPLES

4.1. Parallel-plate Waveguide Filled with a DPS/DPS (or DNG/DNG) Bilayer

Consider the parallel-plate waveguide filled with a DPS/DPS bilayer of relative material constants $(\epsilon_1, \mu_1) = (4, 2)$ and $(\epsilon_2, \mu_2) = (2, 1.5)$. Dispersion curves are shown in Figs. 2(a) and (b) for the TM and TE modes, respectively. At greater values of v_2 and $\bar{\beta}^2 < \epsilon_2\mu_2$, there are composed modes [19]. As for example, in Fig. 2(a), at $v_2 = 1.5$, the second mode is a compound of $m = 0$ and $m = 1$ modes. Thus, it is more easy to look after the modes starting from the upper region of the dispersion curves, at $\bar{\beta}^2 > \epsilon_2\mu_2$. The cutoffs $\bar{\beta} = 0$ are given by

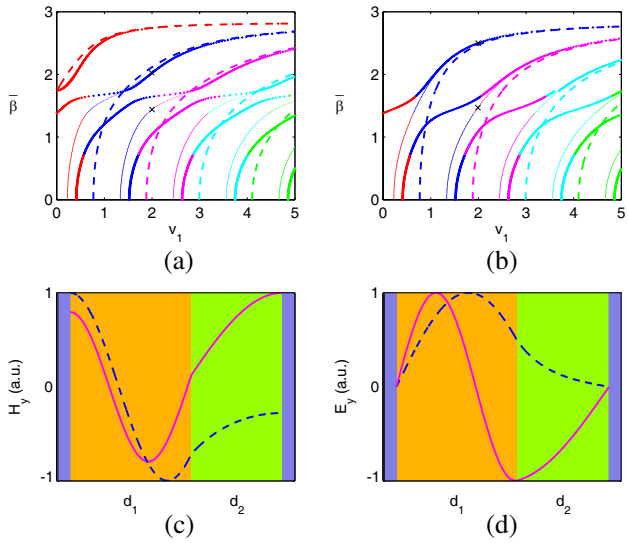

Figure 2. The relative phase constant $\bar{\beta}$ of (a) TM and (b) TE modes in the parallel-plate waveguide filled with a DPS/DPS bilayer of relative material constants $(\epsilon_1, \mu_1) = (4, 2)$ and $(\epsilon_2, \mu_2) = (2, 1.5)$, versus the normalized parameter v_1, when v_2 is constant: $v_2 = 0.5$ (dashed line), $v_2 = 1.5$ (thin line, marker .), and $v_2 = 3$ (thick line, marker +). Only the lower order modes are represented: $m = 0$ (red), $m = 1$ (blue), $m = 2$ (magenta), $m = 3$ (cyan), and $m = 4$ (green). The fields H_y and E_y are represented in (c) and (d), at the points shown in (a) and (b) by black markers, when $v_2 = 1.5$. For the TM modes in (c), $v_1 = 2$, with $\bar{\beta} = 1.44$ (full line), and $\bar{\beta} = 2.03$ (dashed line). For the TE modes in (d), $v_1 = 2$, with $\bar{\beta} = 1.47$ (full line), and $\bar{\beta} = 2.5$ (dashed line).

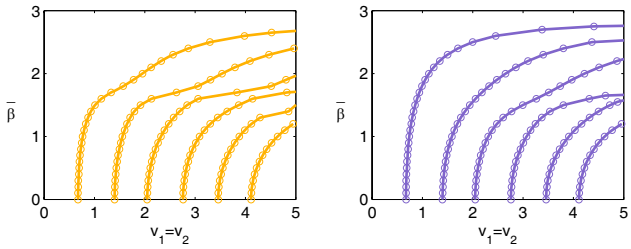

Figure 3. Dispersion curves for (a) TM and (b) TE modes in the parallel-plate waveguide filled with a DPS/DPS bilayer of relative material constants like in Fig. 2, when $v_1 = v_2$.

relation (16) and they are the same for the TM and TE modes. For TM and TE modes, $\bar{\beta}^2$ does not exceed the value $\epsilon_1\mu_1$. In Fig. 2(a), the TM_0 mode has a cutoff $v_1 = 0$ at $\bar{\beta} = \sqrt{\epsilon_2\mu_2} = \sqrt{3}$, which is the same for different values of v_2. At $v_2 = 3$, there is one more cutoff $v_1 = 0$ at $\bar{\beta} = 1.3796$, which is determined from (18) with $l = 1$. That cutoff is the same for the TM and TE polarizations. The fields attain maximum values in the first layer. At $\bar{\beta}^2 > \epsilon_2\mu_2$, the fields are evanescent in the second layer, as shown by the dashed line in Figs. 2(c) and (d).

Note that, for the parallel-plate waveguide filled with a DNG/DNG bilayer of relative material constants $(\epsilon_1, \mu_1) = (-4, -2)$ and $(\epsilon_2, \mu_2) = (-2, -1.5)$, the dispersion curves are the same like in Figs. 2(a) and (b), the single difference being in the sign of the total normalized power $\bar{P}$ carried by the modes on the propagation direction: in the DPS/DPS bilayer $\bar{P} = +1$, the modes representing forward waves, whereas in the DNG/DNG bilayer $\bar{P} = -1$, the modes representing backward waves. Figs. 3(a) and (b) show dispersion curves for the TM and TE modes in the parallel-plate waveguide filled with a DPS/DPS bilayer of relative material constants like in Fig. 2, when $v_1 = v_2$.

4.2. Parallel-plate Waveguide Filled with a DNG/DPS Bilayer

4.2.1. The Case $\epsilon_1\mu_1 > \epsilon_2\mu_2$

Consider the parallel-plate waveguide filled with a DNG/DPS bilayer of relative material constants $(\epsilon_1, \mu_1) = (-4, -2)$ and $(\epsilon_2, \mu_2) = (2, 1.5)$. Dispersion curves are shown in Figs. 4(a) and (b) for the TM and TE modes, respectively. Although the relative material constants differ

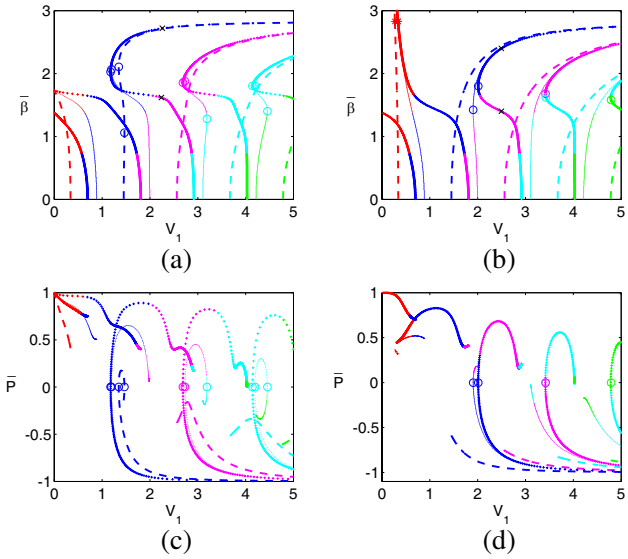

Figure 4. Dispersion curves for (a) TM and (b) TE modes in the parallel-plate waveguide filled with a DNG/DPS bilayer of relative material constants $(\epsilon_1, \mu_1) = (-4, -2)$ and $(\epsilon_2, \mu_2) = (2, 1.5)$, when v_2 is constant: $v_2 = 0.5$ (dashed line), $v_2 = 1.5$ (thin line, marker .), and $v_2 = 3$ (thick line, marker +). The colors are kept the same like in Fig. 2. The TPs are marked by small circles. The total normalized power $\bar{P}$ carried by each mode on the propagation direction is represented in (c) and (d) for the TM and TE modes, respectively.

only by the sign of ϵ_1 and μ_1, the dispersion curves in Fig. 4 are much different from those in Fig. 2. Like in the case of a DPS/DPS bilayer, the dispersion curves overlap in the upper region, at $\bar{\beta}^2 > \epsilon_2\mu_2$, but in the lower region, at $\bar{\beta}^2 < \epsilon_2\mu_2$, there are composed modes. Thus, it is more easy to look after the modes starting from the upper region of the dispersion curves, at $\bar{\beta}^2 > \epsilon_2\mu_2$. The cutoffs $\bar{\beta} = 0$ are given by relation (16) and they are the same for the TM and TE modes. The cutoffs $v_1 = 0$ are the same like in the previous case of a DPS/DPS bilayer. In Fig. 4(b), the TE_0 mode allows real solutions at $\bar{\beta}^2 \geq \epsilon_1\mu_1$, the starting point being marked by an asterisk. At great values of v_2, each TM and TE mode with $m \neq 0$ has at least one TP at which the total power carried on the z direction equals zero and changes the sign. Note that the TPs are more distinctly seen on the $\bar{P}$ against v_1 curves in Figs. 4(c) and (d) than on the dispersion curves. We denote the values of $\bar{\beta}$ and v_1 at the TP by $\bar{\beta}_{\mathrm{TP}}$ and $v_{1_{\mathrm{TP}}}$, respectively. In Fig. 4(a), the

mode TM_1 at $v_2 = 0.5$ has two TPs which are more distinctly seen in Fig. 4(c). Between the two TPs, $\bar{P}$ has positive values. Beyond the two TPs at $m = 1$ and at $m = 2$ and 3, $\bar{P}$ has negative values for the TM modes at $v_2 = 0.5$. At $v_2 = 1.5$, the TM mode with $m = 1$ has one TP, whereas the modes with $m = 2$ and 3 in the upper region have two TPs which are more distinctly seen in Fig. 4(c), $\bar{P}$ having positive values between the two TPs. In Fig. 4(b), at $v_2 = 3$, there is one TP for each TE mode with $m \neq 0$, the TPs at $m = 2$ and $m = 3$ being almost overlapped, but at $v_2 < 3$, there is a single TP for the TE mode with $m = 1$ at $v_2 = 1.5$. The fields H_y and E_y are shown in Figs. 5(a) and (b) for the TM and TE modes, respectively. The behavior of the fields at the DNG-DPS interface is different from that at the interface between the DPS layers in Fig. 2. Fig. 6 shows the dispersion curves of the TM and TE modes in the parallel-plate waveguide filled with a DNG/DPS bilayer of relative material constants like in Fig. 4, when $v_1 = v_2$. The dispersion curves in Figs. 6(a) and (b) are much different from those in Fig. 3. On the same interval of $v_1 = v_2$ variation, in Fig. 6 there are only two modes for each TM or TE polarization, contrary to Fig. 3 which shows a multitude of modes. Each mode of Figs. 6(a) and (b) has a TP at which $\bar{P} = 0$, as shown in Figs. 6(c) and (d), respectively.

4.2.2. The Case $\epsilon_1\mu_1 = \epsilon_2\mu_2$ with $\epsilon_1 = -\epsilon_2$ and $\mu_1 = -\mu_2$

Consider the parallel-plate waveguide filled with a DNG/DPS bilayer of relative material constants $(\epsilon_1, \mu_1) = (-4, -2)$ and $(\epsilon_2, \mu_2) = (4, 2)$. Since the dispersion curves are the same for the TM and TE modes,

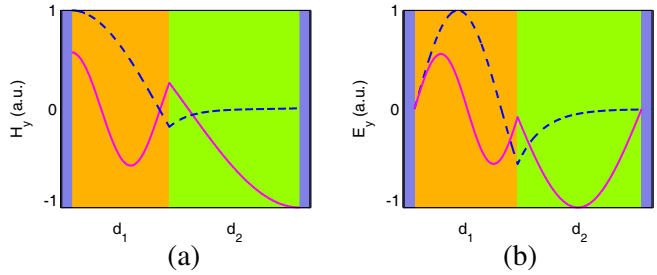

Figure 5. The field H_y in (a) and E_y in (b) for the TM and TE modes in the parallel-plate waveguide filled with a DNG/DPS bilayer at the points shown in Figs. 4(a) and (b) by black markers, when $v_2 = 3$. For the TM mode in (a), $v_1 = 2.25$, with $\bar{\beta} = 1.62$ (full line), and $\bar{\beta} = 2.72$ (dashed line). For the TE mode in (b), $v_1 = 2.5$, with $\bar{\beta} = 1.4$ (full line), and $\bar{\beta} = 2.4$ (dashed line).

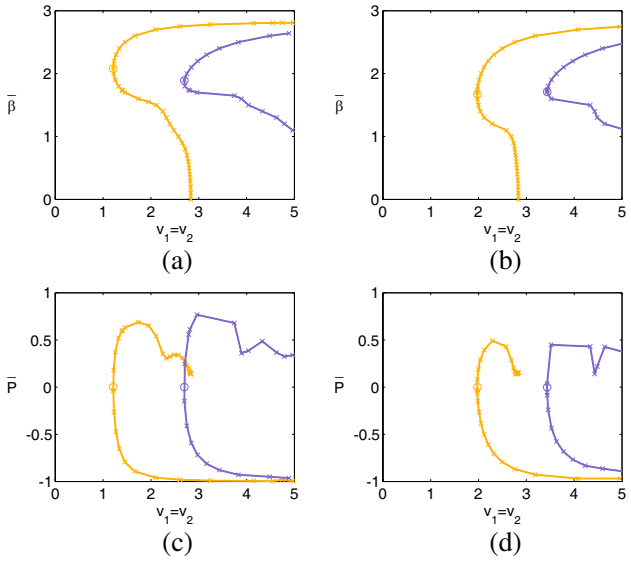

Figure 6. Dispersion curves for (a) TM and (b) TE modes in the parallel-plate waveguide filled with a DNG/DPS bilayer of relative material constants like in Fig. 4, when $v_1 = v_2$. The total normalized power $\bar{P}$ carried by each mode on the propagation direction is represented in (c) and (d) for the TM and TE modes, respectively.

Fig. 7 refers only to the TE modes. A nondispersive mode satisfying relation (20) exists at $v_1 = v_2$, as shown in Figs. 7(a) and (b), which allows any value of $\bar{\beta}$ from 0 to ∞. At $v_1 > v_2$, the total normalized power $\bar{P}$ carried on the propagation direction has negative values (the modes are backward waves), whereas at $v_1 < v_2$, $\bar{P}$ has positive values (the modes are forward waves), as shown in Figs. 7(c) and (d).

4.2.3. The Case $\epsilon_1\mu_1 = \epsilon_2\mu_2$ with $\epsilon_1 = -\mu_2$ and $\mu_1 = -\epsilon_2$

Consider the parallel-plate waveguide filled with a DNG/DPS bilayer of relative material constants $(\epsilon_1, \mu_1) = (-4, -2)$ and $(\epsilon_2, \mu_2) = (2, 4)$. Since the dispersion curves are the same for the TM and TE modes, Fig. 8 refers only to the TE modes. An intricate mode exists at $v_1 \approx v_2$, as shown in Figs. 8(a) and (b), which has two TPs in (a) and four TPs in (b). The total normalized power $\bar{P}$ has positive values between the two TPs of the same order m, as shown in Figs. 8(c) and (d). The modes at $v_1 > v_2$ have $\bar{P} < 0$, whereas the modes at $v_1 < v_2$ have $\bar{P} > 0$. In Fig. 8(c), the mode with $m = 2$ has $\bar{P} \approx 0$ at $v_1 = 3$, but $\bar{P}$ does not change the sign, and so, there is not a TP at that value of v_1.

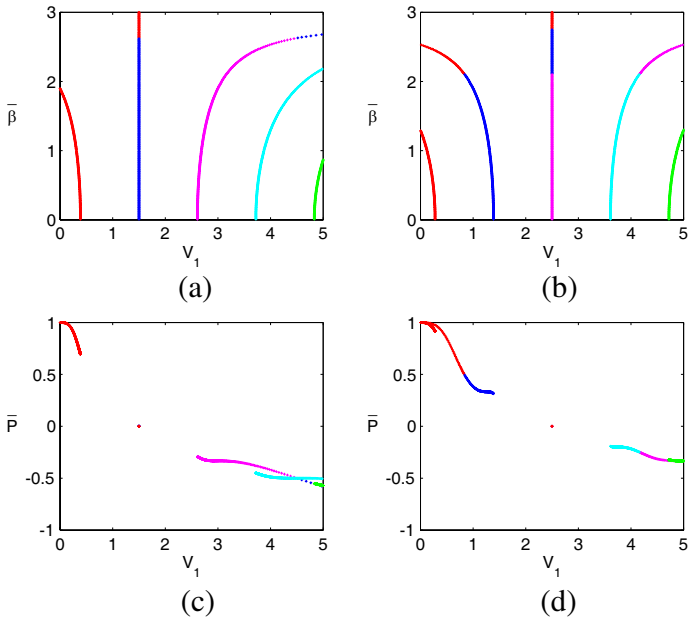

Figure 7. Dispersion curves for the TE modes in the parallel-plate waveguide filled with a DNG/DPS bilayer of relative material constants $(\epsilon_1, \mu_1) = (-4, -2)$ and $(\epsilon_2, \mu_2) = (4, 2)$, when (a) $v_2 = 1.5$ and (b) $v_2 = 2.5$. The total normalized power $\bar{P}$ carried by each mode of (a) and (b), is represented in (c) and (d), respectively.

5. IMPLICIT RELATIONS AT THE TP

Since the TP is an important characteristic of the modes in the parallel-plate waveguide filled with a DNG/DPS bilayer, here we present implicit relations for determining $\bar{\beta}_{\mathrm{TP}}$ when v_2 is constant.

5.1. The Case $\bar{\beta}^2 < \epsilon_2\mu_2 < \epsilon_1\mu_1$

At the TP, v_1 is minimum, and $\mathrm{d}v_1/\mathrm{d}\bar{\beta} = 0$. Since $\mathrm{d}u_1/\mathrm{d}\bar{\beta} \neq 0$, we use relation $\mathrm{d}v_1/\mathrm{d}u_1 = 0$ with the view to finding an implicit relation at the TP. Thus, we obtain the following implicit relation for determining $\bar{\beta}_{\mathrm{TP}}$ when v_2 is constant,

$$\gamma t_2 = \tan\left\{\frac{\gamma}{1+\gamma^2 t_2^2}\left[\sigma\eta t_2 + \frac{u_1^2 v_2}{u_2}\left(1+t_2^2\right)\right]\right\} \tag{27}$$

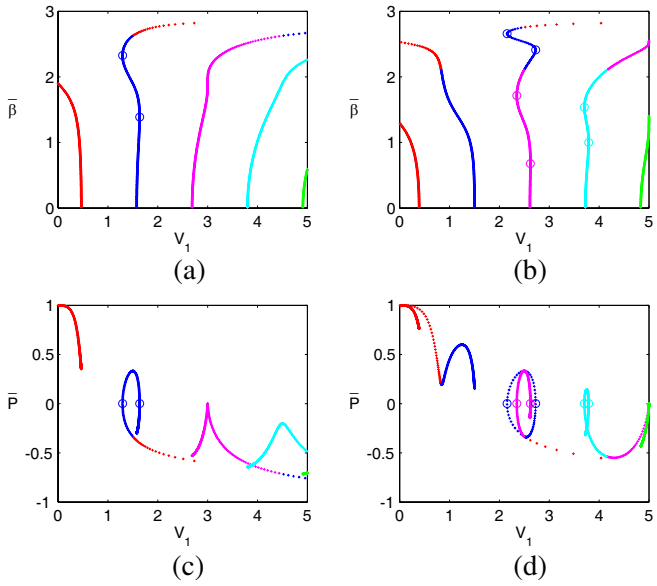

Figure 8. Dispersion curves for the TE modes in the parallel-plate waveguide filled with a DNG/DPS bilayer of relative material constants $(\epsilon_1, \mu_1) = (-4, -2)$ and $(\epsilon_2, \mu_2) = (2, 4)$, when (a) $v_2 = 1.5$ and (b) $v_2 = 2.5$. The total normalized power $\bar{P}$ carried by each mode of (a) and (b), is represented in (c) and (d), respectively.

where γ is defined by relation (15), $t_2 = \tan(u_2 v_2)$, $\eta = 1 - u_1^2/u_2^2$, and

$$\sigma = \begin{cases} -1 & \text{for } TM \text{ modes} \\ 1 & \text{for } TE \text{ modes} \end{cases} \tag{28}$$

Once $\bar{\beta}_{\text{TP}}$ is determined from (27), the respective value $v_{1_{\text{TP}}}$ is obtained from (14).

5.2. The Case $\epsilon_2\mu_2 < \bar{\beta}^2 < \epsilon_1\mu_1$

Using $\mathrm{d}v_1/\mathrm{d}u_1 = 0$ gives the following implicit relation for determining $\bar{\beta}_{\text{TP}}$ when v_2 is constant,

$$\widetilde{\gamma}\tau_2 = \tan\left\{\frac{\sigma\widetilde{\gamma}}{1+\widetilde{\gamma}^2\tau_2^2}\left[\widetilde{\eta}\tau_2 - \sigma\frac{u_1^2 v_2}{\widetilde{u}_2}\left(1-\tau_2^2\right)\right]\right\} \tag{29}$$

where $\widetilde{\gamma}$ is defined by relation (24), $\tau_2 = \tanh(\widetilde{u}_2 v_2)$, $\widetilde{\eta} = 1 + u_1^2/\widetilde{u}_2^2$. Once $\bar{\beta}_{\text{TP}}$ is determined from (29), the respective value $v_{1_{\text{TP}}}$ is obtained from (23).

5.3. The Case $\epsilon_1\mu_1 = \epsilon_2\mu_2$ with $\epsilon_1 = -\mu_2$ and $\mu_1 = -\epsilon_2$

Replacing $u_1 = u_2$ and $\eta = 0$ in (27) gives the following implicit relation for determining $\bar{\beta}_{\mathrm{TP}}$ of the TM and TE modes, when v_2 is constant,

$$\gamma t_2 = \tan\left[\gamma u_1 v_2 \left(1 + t_2^2\right) / \left(1 + \gamma^2 t_2^2\right)\right] \tag{30}$$

where $\gamma = \epsilon_1/\mu_1$.

5.4. Numerical Examples

Using relations (27) and (29) gives at $v_2 = 1.5$ in Fig. 4(a) $[\bar{\beta}_{\mathrm{TP}}, v_{1_{\mathrm{TP}}}] = [2.0646, 1.1977]$ at $m = 1$, $\bar{\beta}_{\mathrm{TP}} = [1.8779, 1.2771]$ with $v_{1_{\mathrm{TP}}} = [2.7343, 3.1907]$ at $m = 2$, and $\bar{\beta}_{\mathrm{TP}} = [1.7993, 1.4003]$ with $v_{1_{\mathrm{TP}}} = [4.1942, 4.4539]$ at $m = 3$, the values of m referring to the upper region of the dispersion curves. Using relation (30) gives for the TPs in Fig. 8(a) $\bar{\beta}_{\mathrm{TP}} = [1.3882, 2.3246]$ with $v_{1_{\mathrm{TP}}} =$

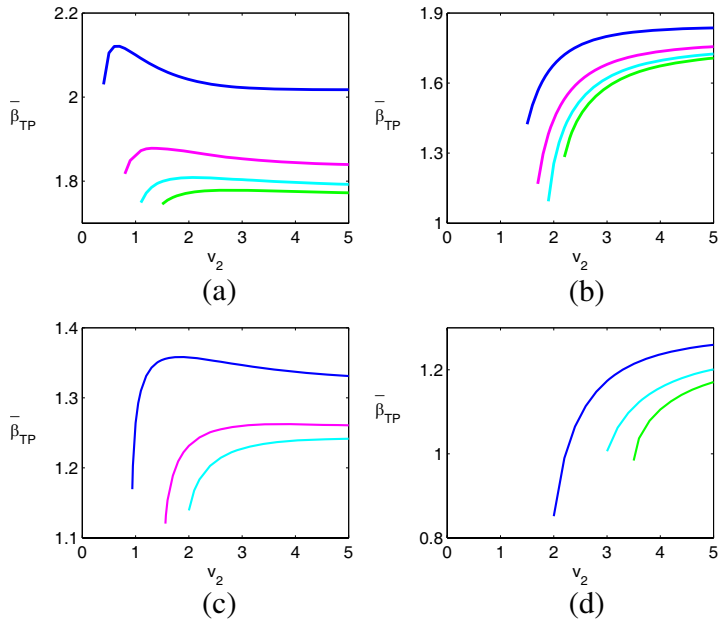

Figure 9. The relative phase constant $\bar{\beta}_{\mathrm{TP}}$ versus v_2 for (a) TM and (b) TE modes in the parallel-plate waveguide filled with a DNG/DPS bilayer of relative material constants like in Fig. 4, that is, $(\epsilon_1, \mu_1) = (-4, -2)$ and $(\epsilon_2, \mu_2) = (2, 1.5)$. The same in (c) and (d), but for the relative material constants $(\epsilon_1, \mu_1) = (-2, -1.5)$ and $(\epsilon_2, \mu_2) = (1.5, 1)$.

$[1.6368, 1.2940]$, whereas in Fig. 8(b), for the intricate mode at $v_1 \approx v_2$, $\bar{\beta}_{\mathrm{TP}} = [2.6581, 2.4112, 1.7149, 0.6780]$ with $v_{1_{\mathrm{TP}}} = [2.1566, 2.7280, 2.3495, 2.6235]$, and for the next mode on the side $v_1 > v_2$ in that figure, $\bar{\beta}_{\mathrm{TP}} = [1.5376, 0.9988]$ with $v_{1_{\mathrm{TP}}} = [3.7055, 3.7899]$. The dependence of $\bar{\beta}_{\mathrm{TP}}$ on v_2 is illustrated in Fig. 9 for two sets of relative material constants, with $\epsilon_1\mu_1 > \epsilon_2\mu_2$. When two TPs there are for a given mode, the principal TP corresponding to the maximum value of $\bar{\beta}_{\mathrm{TP}}$ is considered. The TP appears at certain values of v_2, the higher is the mode order, the greater is the v_2 parameter at which the TP begins to exist. One can see that the behavior of the TPs is different for the TM and TE modes. In Fig. 9(d), the TPs at $m = 2$ and $m = 3$ are overlapped.

6. CONCLUSION

In this paper, we analyzed the TM and TE modes of the parallel-plate waveguide filled with DPS/DPS (or DNG/DNG), and DNG/DPS bilayers. Simple normalized dispersion relations for the guided and evanescent modes were presented. Numerical examples were given showing dispersion curves, the total normalized power carried by the modes on the propagation direction, and the fields inside the parallel-plate waveguide. Interesting results were obtained in the specific case when $\epsilon_1\mu_1 = \epsilon_2\mu_2$, as for example, the nondispersive mode in Fig. 7, at $v_1 = v_2$, and the intricate mode in Fig. 8, at $v_1 \approx v_2$. Although the TP has been evidenced by other authors [9, 15], there is no relation (upon our knowledge) for the normalized parameters at the TP. In this paper we presented implicit relations for determining the normalized parameters at the TP for the TM and TE modes in the parallel-plate waveguide filled with a DNG/DPS bilayer. We showed that the TP appears at certain values of the DPS layer parameter v_2, the higher the mode order, the greater the v_2 parameter at which the TP begins to exist. The behavior of the TP is different for the TM and TE modes, as shown in Fig. 9. We showed also that a given mode could have several TPs, as for example, the intricate mode in Fig. 8(b) at $v_1 \approx v_2$ has four TPs, the plots of the total normalized power carried by each mode on the propagation direction being very useful in the designation of the TPs. For simplicity, we considered $\epsilon_1\mu_1 \geq \epsilon_2\mu_2$ and several examples were given, but relations presented in terms of normalized parameters in this paper could be applied also to other combinations for the relative material constants of the DPS and DNG materials [13].

REFERENCES

1. Veselago, V. G., "The electrodynamics of substances with simultaneously negative values of permittivity and permeability," *Sov. Phys. Usp.*, Vol. 10, 509–514, 1968.
2. Shelby, R. A., D. R. Smith, and S. Schultz, "Experimental verification of a negative refractive index of refraction," *Science*, Vol. 292, 77–99, 2001.
3. Pendry, J. B., "Negative refraction makes a perfect lens," *Phys. Rev. Lett.*, Vol. 85, 3966–3969, 2000.
4. Smith, D. R. and N. Kroll, "Negative refraction index in left handed materials," *Phys. Rev. Lett.*, Vol. 85, 2933–2936, 2000.
5. Ziolkowski, R. W. and E. Heyman, "Wave propagation in media having negative permittivity and permeability," *Phys. Rev. E*, Vol. 64, 056625, 2001.
6. Lindell, I. V., S. A. Tretyakov, K. I. Nikoskinen, and S. Ilvonen, "BW media-Media with negative parameters, capable of supporting backward waves," *Microwave Opt. Technol. Lett.*, Vol. 31, 129–133, 2001.
7. Lindell, I. V. and S. Ilvonen, "Waves in a slab of uniaxial BW medium," *Journal of Electromagnetic Waves and Applications*, Vol. 16, No. 3, 303–318, 2002.
8. Kong, J. A., "Electromagnetic wave interaction with stratified negative isotropic media," *Progress In Electromagnetics Research*, Vol. 35, 1–52, 2002.
9. Nefedov, I. S. and S. A. Tretyakov, "Waveguide containing a backward-wave slab," *Radio Science*, Vol. 38, 1101, 2003.
10. Wu, B.-I., T. M. Grzegorczyk, Y. Zhang, and J. A. Kong, "Guided modes with imaginary transverse wave number in a slab waveguide with negative permittivity and permeability," *J. Appl. Phys.*, Vol. 93, 9386–9388, 2003.
11. Shadrivov, I. V., A. A. Sukhorukov, and Y. S. Kivshar, "Guided modes in negative-refractive-index waveguides," *Phys. Rev. E*, Vol. 67, 057602, 2003.
12. Peacock, A. C. and N. G. R. Broderick, "Guided modes in channel waveguides with a negative index of refraction," *Opt. Express*, Vol. 11, 2502–2510, 2003.
13. Alu, A. and N. Engheta, "Guided modes in a waveguide filled with a pair of single-negative (SNG), double-negative (DNG), and/or double-positive (DPS) layers," *IEEE Trans. Microwave Theory Tech.*, Vol. 52, 199–210, 2004.

14. Ran, L.-X., H.-F. Jiang Tao, H. Chen, X.-M. Zhang, K.-S. Cheng, T. M. Grzegorczyk, and J. A. Kong, "Experimental study on several left-handed metamaterials," *Progress In Electromagnetics Research*, Vol. 51, 249–279, 2005.
15. Mahmoud, S. F. and A. J. Viitanen, "Surface wave character on a slab of metamaterial with negative permittivity and permeability," *Progress In Electromagnetics Research*, Vol. 51, 127–137, 2005.
16. Li, C., Q. Sui, and F. Li, "Complex guided wave solution of grounded dielectric slab made of metamaterials," *Progress In Electromagnetics Research*, Vol. 51, 187–195, 2005.
17. Xiao, Z. Y. and Z. H. Wang, "Dispersion characteristics of asymmetric double-negative material slab waveguides," *J. Opt. Soc. Am. B*, Vol. 23, 1757–1760, 2006.
18. Tsakmakidis, K. L., C. Hermann, A. Klaedtke, C. Jamois, and O. Hess, "Surface plasmon polaritons in generalized slab heterostructures with negative permittivity and permeability," *Phys. Rev. B*, Vol. 73, 085104, 2006.
19. Wang, Z. H., Z. Y. Xiao, and S. P. Li, "Guided modes in slab waveguides with a left handed material cover or substrate," *Opt. Commun.*, Vol. 281, 607–613, 2008.
20. McCall, M. W., "What is negative refraction?" *Journal of Modern Optics*, Vol. 56, 1727–1740, 2009.
21. Yang, H. W., P. Dong, and Y. Liu, "Transmission properties of asymmetric slab waveguides with left-handed materials," *J. Russ. Laser Res.*, Vol. 30, 193–203, 2009.
22. Dong, P. and H. W. Yang, "Guided modes in slab waveguides with both double-negative and single-negative materials," *Optica Applicata*, Vol. 40, 873–882, 2010.
23. Cojocaru, E., "Electromagnetic tunneling in lossless trilayer stacks containing single-negative metamaterials," *Progress In Electromagnetics Research*, Vol. 113, 227–249, 2011.
24. Lindell, I. V. and A. H. Sihvola, "Electromagnetic boundary and its realization with anisotropic metamaterial," *Phys. Rev. E*, Vol. 79, 026604, 2009.